Metallocene Polyolefins and Their Blends[#]

Michael Hess

Department of Physical Chemistry, Gerhard-Mercator-University
D-47048 Duisburg, Germany

Betty Lucy Lopez[*] *and Carmina Gartner*

Departemento de Quimica, Universidad de Antioquia, Apartado Aereo 1226
Medellin, Colombia, South America

SUMMARY: Commercial copolymers of 1-octene and ethylene: metallocene catalyzed (mLLDPE) and Ziegler-Natta catalyzed (znLLDPE), a low density polyethylene (LDPE), and high density polyethylene (HDPE), were characterized with respect to branching, crystallization behaviour and dynamic-mechanical properties. It was found that the crystallinity of the polymers is more influenced by the homogeneity of the short-chain branching than by its content. The study of blends of mLLDPE and znLLDPE with LDPE and HDPE showed that the interaction between mLLDPE and LDPE is stronger than between znLLDPE and LDPE. Blends containing mLLDPE showed a composition depending improvement of the storage modulus G' which was not observed in znLLDPE/LDPE blends. The HPDE blends followed a linear mixing rule. Co-crystallization was found mLLDPE/LDPE and partially in znLLDPE/LDPE and znLLDPE/HDPE blends, respectively.

Introduction

The discovery of metallocene-catalyzed polymerization of α-olefins[1] has opened a great variety for the synthesis of new materials with controlled stereoregularities, molar mass and molar mass distribution, and for copolymerization. The properties of commercial polyethylens (PE), copolymers or blends depends not only on the chemical structure but also on the manufacturing process and the thermal history.

The most important PEs are low density polyethylenes (LDPE), linear low density polyethylenes (LLDPE), and high density polyethylenes (HDPE). HDPE comprises regular chains with typically less than 7 branching points per 1000 chain carbons, a melting temperature $T_m > 130°C$. They are highly crystalline with a density $\rho = 0.94...0.97$ g/cm^3 and a yield stress $\sigma_y \cong 43$ MPa. LDPEs are highly branched polymers with typically 60 branching points per 1000 chain carbons, a melting temperature T_m of about 110°C. The crystallinity is significantly lower than in HDPE, so that the density is around $\rho = 0.92$ g/cm^3 and a yield

[#] dedicated to Prof. (em) Dr. Robert Kosfeld, Aachen, on the occasion of his75th birthday.
[*] To whom correspondence should be addressed

 CCC 1022-1360/00/$ 17.50+.50/0

stress $\sigma_y \cong 24$ MPa. LLDPEs are copolymers of ethen and α-olefines such as butene-1, pentene-1, hexene-1 or octene-1. The melting point T_m is around 120°C...130°C, with a density $\rho = 0.92...0.94$ g/cm^3 and a yield stress $\sigma_y \cong 37$ MPa. The branching can be controlled. The hardness is higher while its brittleness temperature is lower compared with LDPE, so that substitution of LDPE by LLDPE becomes more and more popular. Therefor, it is of great interest to know in which way the properties of LLDPE depend on synthesis.

Fractionation – in particular the temperature-rising-fractionation[2] (TREF) – and crystallization behaviour in combination with IR-spectroscopic studies are suited to provide information about short-chain branching and its homogeneity and hence about the chemical micro-structure. Fractionated crystallization[3,4,5,6,7] reflects the molecular heterogeneity through the thickness of the crystalline lamellae which depend on thermal history and composition[8]. Blending of polyolefins can show synergistic effects in physical properties of materials such as modulus, toughness or processability. Since different catalysts influence the micro-structure of the polymers, this can affect miscibility and the behaviour of blends, in particular when both components are crystallizable. In these cases 4 types according to crystallization and miscibility can be discriminated[9]: miscibility or immiscibility in the amorphous state and co-crystallization or separate crystallization. Stein[10,11,12]and coworkers have conducted extensive studies of polyolefin blends using calorimetric and scattering techniques. They have observed no segregation in crystalline structures of LLDPE/HDPE blends, while LLDPE/LDPE blends suggest formation of separate crystal. The LLDPE was an ethylene butene-1 copolymer. We wanted to study the influence of longer side-chains (octyl-) in blends containing metallocene-catalyzed linear low density polyethylenes (mLLDPEs) or Ziegler-Natta-catalyzed linear low density polyethylenes (znLLDPEs) and conventional low density polyethylene (LDPE) or high density polyethylene (HDPE) using ubiquitous commercial polymers.

Materials and Methods

mLLDPE: Affinity 1881, Dow Chemicals, metallocene catalyzed, with 12% 1-octene copolymerized, $\rho = 0.903$ g/cm^3, melt flow index MFL = 1.0 g/10 min

znLLDPE: Dowlex NG2085, Dow Chemicals, Ziegler-Natta-catalyzed 1-octene copolymer, $\rho = 0.92$ g/cm^3, melt flow index MFL = 0.915 g/10 min

LDPE: Polifen 641, Policolsa, high pressure polymerized, branched homopolymer, $\rho = 0.92$ g/cm^3, melt flow index MFL = 2.0 g/10 min

HDPE: Altaven 5200B, Plásticos del Lago, organometallic catalyzed linear homopolymer, $\rho = 0.97$ g/cm^3, melt flow index MFL = 0.35 g/10 min

For comparison also an isotactic polypropylene (iPP) was used:

iPP: 01H41, Propilco, Ziegler-Natta catalyzed homopolymer 96% isotactic, $\rho = 0.915$ g/cm^3, melt flow index MFL = 1.4 g/10 min

The molar mass distribution of the samples was not available for this investigation. All samples were, however, prepared from the same master batch so that they are comparable among each other.

Blending: Blends with the indicated composition were prepared within 5 min in a Haake torque rheometer using sigma rollers at 60 rpm, 180°C.

IR-Spectroscopy: A Perkin-Elmer FTIR-Spectrometer (Spectrum 1) was used to determine the short-chain branching content (SCBC) according to ASTM D-2238-68 using specimens prepard from compressed and quenched films. The 1378 cm^{-1} methyl C-H vibration was used after deconvolution of the bands at 1367 cm^{-1} and 1350 cm^{-1} (short methylene sequences in non-planar conformations) and calibration with standard substances. Sample thickness was corrected with the intensity of the C-C skeletal vibration in the crystalline phase at 2019 cm^{-1}.

Calorimetry: TA-Instruments 2920 and Perkin Elmer DSC 7

WAXS: Bruker AXS D8 at 40 kV, 30 mA, from $2\theta = 2°$ ...40° (Cu and Ni). The counts at $2\theta = 21°$ (110 plane of the orthorhombic elementary cell) and $2\theta = 23°$ (200 plane of the elementary cell) were taken as a relative measure of the crystallinity of the samples.

Dynamic-Mechanic Analysis (DMTA): Torsion Pendulum[13, 14], ATM-3, Fa. Myrenne, Roetgen, Germany, measuring frequency used 1 Hz in the temperature range from –180°C to 100°C. The heating rate was 2°C/min. The strip-shaped specimens were moulded at 180°C and cooled down to room temperature within 45 min under a pressure of approximately 150 MPa.

TREF-Analysis: The step-wise fractionation followed the method described by Fan e.a.[15]. About 2g polymer was dissolved in 200 mL boiling xylene. The solution was cooled down with 10°/h to room temperature the fractionation temperature (25°C, 50°C, 75°C, and 100°C) and kept there for 24hrs. Each fraction was collected by centrifugation and analyzed by DSC and spectroscopically.

Fractionated Crystallization: The polymers were heated up in the DSC well into the molten state and kept there for 3 min under nitrogen. The samples were then cooled down to the starting temperature T_{start} (see Table 1) and kept there for 150 min. After that time, the

samples were cooled down 6°C with a cooling rate of 10°C/min, kept there for 150 min and so forth until the end temperature T_{end} (see Table 1) was reached. After these steps of secondary crystallization, the samples were analyzed by a heating rum with a rate of 5°C/min.

Table 1: Start-and end-temperatures for secondary crystallization.

polymer	T_{start}/°C	T_{end}/°C
mLLDPE	116	56
znLLDPE	128	68
LDPE	122	62
HDPE	134	74

Results and Discussion

The Pure Components

DMTA reveals three main thermal transitions in PE, called α-, β-, and γ-process in decreasing order from high temperatures, see Fig. 1.

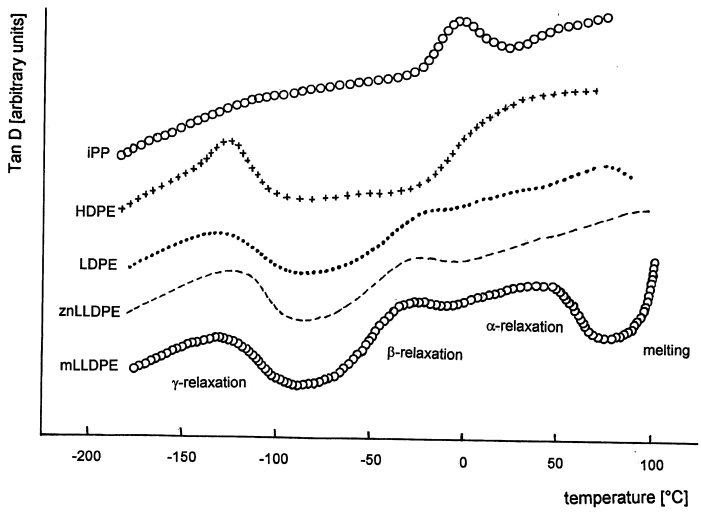

Figure 1. DMTA of the pure PEs. iPP shows no γ-transition, its glass transition temperature is at 0°C.

The α-process is associated with a longitudinal chain transport in the crystalline phase caused by 180° rotations[16]. It is usually the strongest relaxation in PE at 50°C and higher. The β-

process is localized around –35°C and associated with the glass transition[17]. This transition is usually broad and week. Frequently, in particular in HDPE, it is almost invisible and appears only in the swollen state. It becomes stronger upon branching. The γ-transition is of complex, composite structure, interpreted as a kink-inversion[18], or as molecular motions in longer loops by local reorientations of short methylene units in crystalline phases, motions near crystalline defects[17].

Fig. 1 shows the damping factor Tan D, which is the quotient of the loss-modulus G" and the storage modulus G', and has the physical meaning of the phase shift between stress and corresponding deformation. mLLDPE, znLLDPE, and LDPE show a clear, broad β-relaxation, whereas HDPE only shows a very weak and broad deviation from the base line at-50°C. This transition becomes more pronounced – even in HDPE – if the sample contains a solvent like CCl_4. The composite structure of the γ-process is clearly visible and shows a different shape in all samples. The α-process is broad and the most prominent in HDPE near 50°C. The low density PEs mainly show an increasing damping up to 100°C, only mLLDPE shows a clear maximum near 50°C.

IR-spectroscopic analysis revealed that vinyl (906 cm^{-1}, 990 cm^{-1}), vinyliden (888 cm^{-1}) and vinylen trans double bonds (960-966 cm^{-1}) were present in **mLLDPE**. The glass transition temperature was determined from the β-transition of DMTA-experiments around –36°C. The γ-transition with a broad maximum at –136°C was the lowest of all samples. The melting transition was broad with a maximum at 101°C and a shoulder at 69°C (DSC), $\Delta_{fus}H = 65$ J/g.

The number of vinylidene-type double bonds was higher in **znLLDPE** compared with mLLDPE. The amount of vinyl-terminal groups, however was smaller. This is characteristic for Ziegler-Natta-type linear low density PEs. The β-transition occurred at –33°C. There were two melting peaks indicating segregation into two crystalline populations at 110°C and 124°C with a total heat of fusion $\Delta_{fus}H = 94$ J/g.

The number of vinylidene-type double bonds is much higher and the number of vinyl end groups is much smaller in **LDPE** compared with the linear low density PEs. The glass temperature at the maximum of the β-transition (Tan D) is at –25°C. There is only one melting point at 114°C with $\Delta_{fus}H = 100$ J/g.

The IR-spectrum of **HDPE** is very similar to znLLDPE, however, the methyl group absorptions are very weak. The glass transition is very weak, localized around –50°C. The melting occurrs in a narrow temperature range with only one maximum at 137°C and a high crystallinity, $\Delta_{fus}H = 231$ J/g.

In order to obtain some information about the microstructure of the pure polymers, the short chain branching was determined by IR-spectroscopy after extraction at four different temperatures (discontinuous TREF). It was not possible so far to study the microstructure by more sophisticated methods like NMR, this will be subject of future investigations, especially since they will provide more information about the amorphous regions, chain segment mobility and crystalline defects[19]. The TREF results are given in Table 2.

Table 2: Extraction experiments.

Polymer	extraction temperature [°C]	mass fraction [%]	Tm [°C]	CH_3/1000C	counts 2 theta 21°	counts 2 theta 23°
mLLDPE	25	3	98	14	50	18
	50	17	100	5,5	50	18
	75	72	103	1,8	95	20
	100	7	102	4,6	80	20
	100		84			
znLLDPE	25	4	74	15	40	10
	25		114			
	50	5	92	0,9	40	10
	50		121			
	75	20	90	1,8	110	20
	75		107			
	100	53	122	1,9	100	30
	100		109			
	insoluble	17	126	0,9	180	40
LDPE	25	3	103	2,6	130	30
	25		91			
	50	4	103	48	170	40
	50		92			
	75	44	109	0,26	180	40
	100	48	113	9,6	140	40
HDPE	25	1	126	0,13	40	90
	25		80			
	50	6	134	0,36	300	90
	75	15	136	0,21	310	90
	100	70	132	0,32	320	90
	insoluble	8	135	0,11	290	90

Table 2 shows the TREF-Analysis of the polyethylenes combined with a IR-spectroscopic-, calorimetric-and WAXS-analysis, which yield information about SCBC, melting and the crystalline phases, respectively. The integrals over $2\theta = 21°$ and $2\theta = 23°$ after corrections is a measure of the crystallinity.

In general it can be stated that those PEs with a high SCBC shows a high solubility at low temperatures. These fractions show usually a low crystallinity and a low melting point indicating steric ramifications and crystalline defects caused by the high concentration of side-chains. WAXS-analysis shows that the amorphous halo is much more pronounced in mLLDPE and znLLDPE compared with the other polymers where it is rather weak. The TREF-experiment is relatively insensitive against influences of the molar mass of the polymers according to Wild e. a.[20] as long as the molar masses are > 1000 g/mol. Material with M< 500 g/mol is usually soluble at room temperature in xylene. Since the fractionation was discontinuous with rather broad temperature steps the SCBC values given in Table 2 are average values.

mLLDPE and znLLDPE have high amounts of fractions with a low short-chain branching. LDPE shows the highest amount of short-chain branching, while HDPE shows practically no short-chain branching. LDPE shows a rather inhomogeneous SCBC distribution as shown in Fig. 2 and Fig. 3.

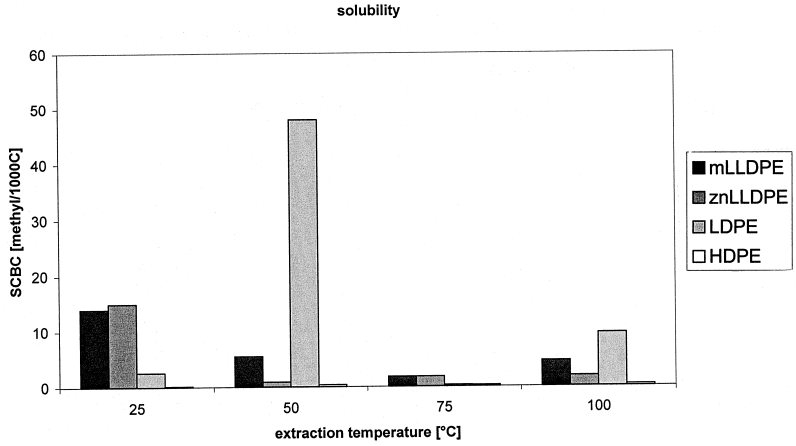

Figure 2. SCBC distribution from extraction at four temperatures (25°C, 50°C, 75°C, and 100°C). The corresponding mass distribution is shown in Fig. 3.

Short-chain branching is almost negligible in HDPE. At low extraction temperatures only small amounts of material are soluble which show – except for LDPE – the highest SCBC. In general, SCBC decreases with increasing temperature while the mass fraction of the extracted material increases with temperature. Most of the material is soluble at the highest temperature used in these experiments. There are two exceptions: most of the mLLDPE (72%) is extracted at 75°C and only 7% at 100°C; the fraction extracted from LDPE at 50°C contains the highest

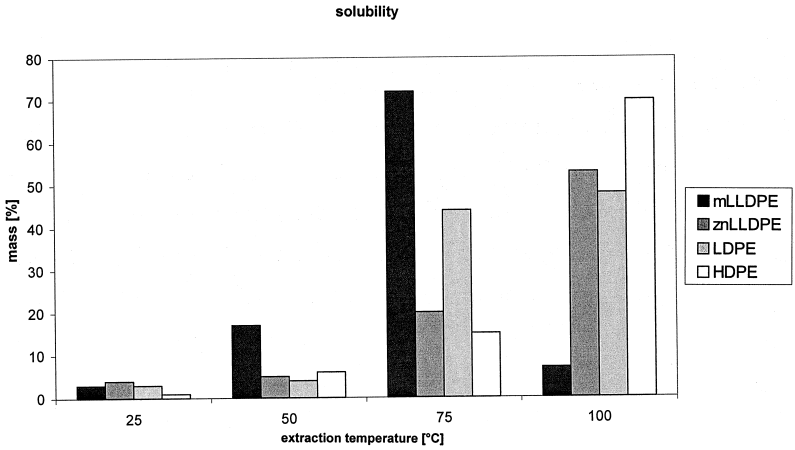

Figure 3. Mass distribution from extraction at 25°C, 50°C, 75°C, and 100°C.

SCBC (48%). While mLLDPE is completely soluble at 100°C, 17% znLLDPE with high crystallinity and with a high melting point and low SCBC remain insoluble at 100°C. Since znLLDPE of about the same SCBC is soluble already at 50°C, the reason for this behaviour is probably a higher molar mass with larger crystals or a block formation. A much higher molar mass of the znLLDPE may be the more probable explanation, since only 8% of the HDPE with a much higher melting point and a higher degree of crystallinity and almost no branching are insoluble at 100°C.

The differences in the melting behaviour of the material which can be extracted from one sample at different temperatures is shown in Fig. 4. Characteristics are the melting point (quality of the crystals), the width of the melting peak (uniformity of the crystalline material), area under the peak (amount of crystalline phase), and the existence of shoulders and/or additional peaks. Inhomogeneities of the distribution of the crystal populations can be found in particular in znLLDPE and LDPE.

The thermal history applied to the samples during the fractionated crystalization causes the co-called "secondary crystallization". While this phenomenon is not observed in HDPE and PP, two different mechanisms are known for LDPE on one side and mLLDPE and znDPE on the other side. As shown by Strobl[21], [22] e. a. by measurements of the interfacial area of the crystalline material per unit volume annealing causes surface crystallization in LDPE, while in mLLDPE and znLDPE insertion is observed, which means that new crystalline layers are formed between the layers of sperulitic material. The melting endotherms of mLLDPE, znLLDPE and LDPE are shown in Fig. 5. HDPE only shows one single melting endotherm.

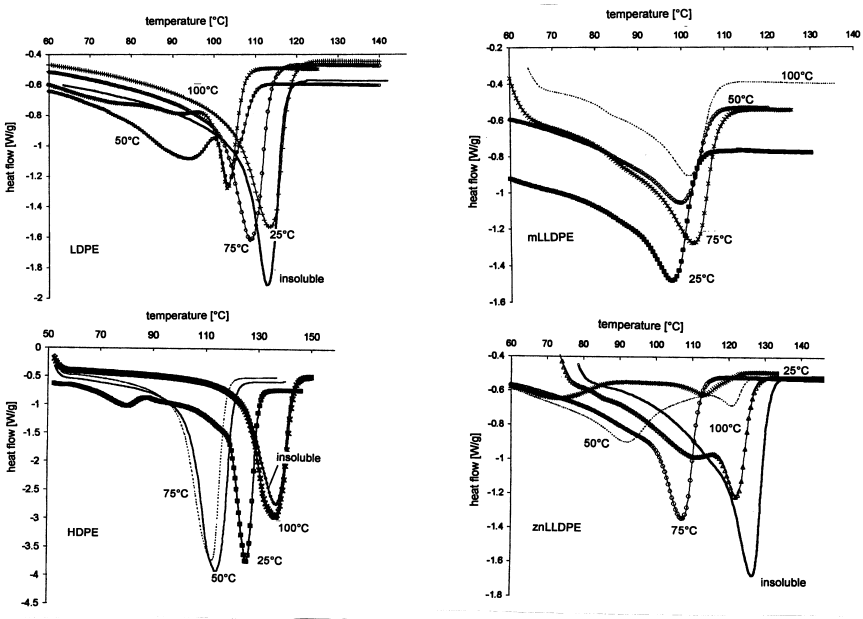

Figure 4. DSC-trace of the material extracted at the indicated temperatures and the insoluble.

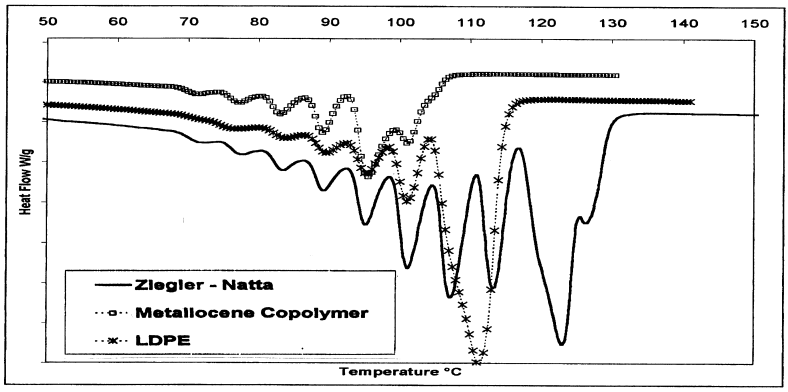

Figure 5. DSC-traces of znLLDPE, mLLDPE, and LDPE after secondary crystallization. HDPE and PP are not shown since they show no such effect.

After annealing according to the temperature program given in the Section Materials and Methods, all low density polyethylenes show multiple melting endotherms indicating different crystalline populations, distribution of crystals and molar mass related to the corresponding SCBC. The analysis of the calorimetric in terms of T_m and the crystallinity calculated from $\Delta_{fus}H$ are given in Table 3. The highest melting endotherm for mLLDPE was 101°C. Longer annealing at higher temperatures did not change the results which means that

there are no longer sequences are present than those melting at 101°C. znLLDPE shows more melting endotherms than the metallocene-catalyzed PE. The mass distribution of the crystalline material reflects its heterogeneity. mLLDPE and znLLDPE show a very similar secondary crystallization, however, the crystal populations in znLLDPE melting at 113°C, 123°C, and 127°C are completely absent in mLLDPE, that one melting at 107°C shows only a weak shoulder in the DSC trace. The melting endotherms of LDPE are generally broader compared with the linear low density polyethylenes. The population melting at 71°C is practically missing and the next two are shifted to slower temperatures. Those melting at 95°C and 101°C are the same as in znLLDPE but the strongest population melting at 111°C is not present in the LLDPEs.

Table 3. Secondary crystallization.

Material	T_m/°C	Fraction of the total crystallinity [%]
mLLDPE	71.0	3
	77.1	5
	83.1	10
	89.1	21
	95.3	48
	101.3	13
znLLDPE	71.3	0.8
	77.0	1
	83.0	2
	89.0	4
	95.0	7
	101.1	13
	107.1	18
	113.3	17
	122.9	34
	126.6	4
LDPE	75.9	0.9
	83.4	1
	89.5	2
	95.3	5
	101.1	9
	111.4	82
HDPE	137.3	100
PP	167.8	100

Another crystalline population only present in one polymer is the one melting between 118°C and 130°C in znLLDPE. It shows a complex composition with at least three different components.

Binary Blends

The System mLLDPE/LDPE:

Both of the pure components show only one relatively broad melting transition, 101°C and 113°C, respectively, corresponding to the strongest crystalline population formed by fractionated crystallization, see Table 3. The glass transition temperatures of the pure components estimated from the broad β-transition in the dynamic–mechanical experiment differ significantly. The behaviour of the blends is summarized in Fig. 6.

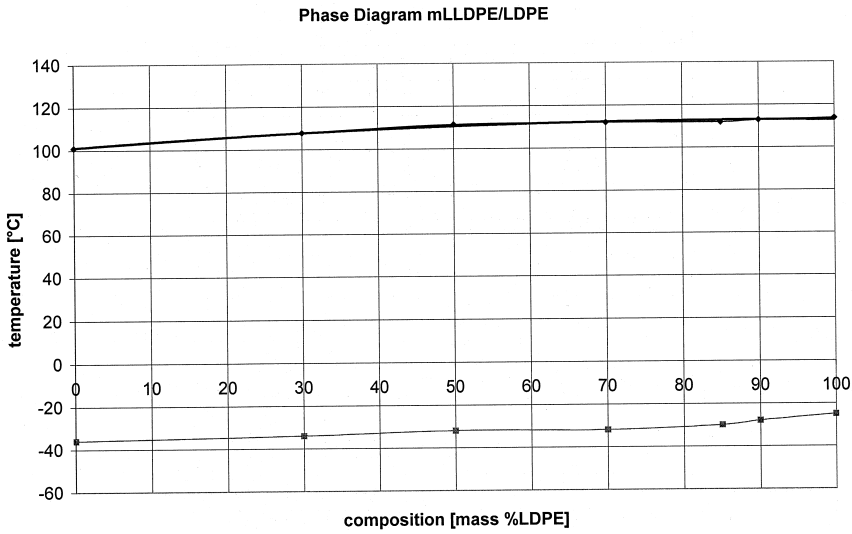

Figure 6. Phase diagram of mLLDPE and LDPE. Melting point from calorimetry, glass transition temperature from DMTA (maximum of the β-process of Tan D, the damping).

There is only one melting process starting at the melting temperature of pure mLLDPE (101°C) ending at the melting temperature of the pure LDPE (113°C). The peak positions of the blends shift depends on the composition and can be described with good accuracy by a second order polynomal. The peak width at ½ of the melting peak height remains almost constant within experimental error without significant minima or maxima.

The storage modulus G'(T), Fig. 7, and the damping Tan D of the blends are always between the values of the pure components. The γ-process is very similar in both pure components and there is no significant composition dependence. The β-process and the α-process are significantly depending on the composition and are always between the values of the pure components. The density of the blend increases from ρ(25°C) = 9.02 g/cm^3 (mLLDPE) to the value of the pure LPDE ρ (25°C) = 9.15 g/cm^3 in an increasing curve without maximum. In accordance with the results published by Stein and coworkers [10-12] this can be interpreted as cocrystallization of mLLDPE and LDPE.

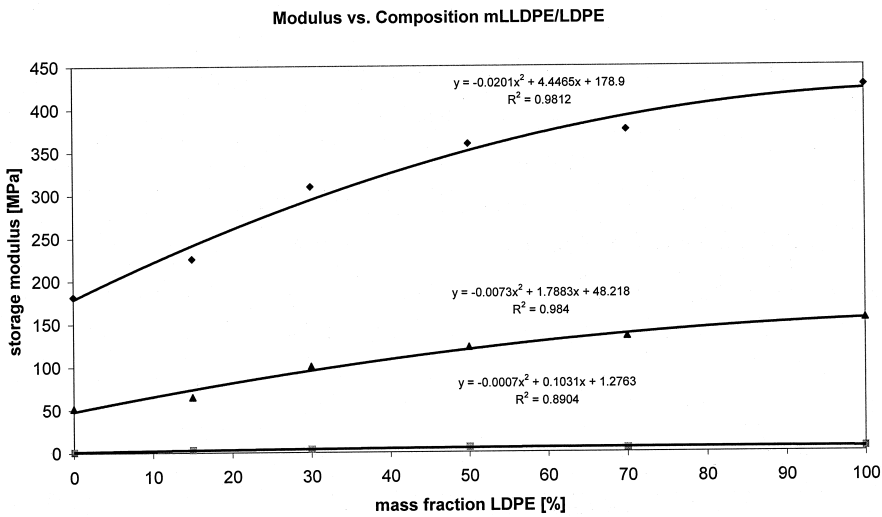

Figure 7. Composition-dependence of the storage modulus G' at –20°C (■), 20°C (▲) and 100°C (◆) in mLLDPE/LDPE blends. The curves can be fitted by a second order polynomal.

The System mLLDPE/HDPE:

While the pure components only show one melting endotherm, the blends show both of them over the whole concentration range which are depending on the composition, Fig. 8. The melting points are slightly decreasing. This is a clear indication that the two components crystallize separately. There is only one glass transition temperature visible which increases with increasing amount of HDPE. The glass (β-) transition of pure HDPE is very weak it cannot be analyzed properly. In the blend, however, there is no trace of it, but the transition is shifterd to higher values with increasing HDPE-content, so that it is very likely that the two components are miscible in the amorphous phase. Dynamic-mechanical analysis shows a

broader and less structured γ-transition and the α-process becomes weaker. The composition dependence of G' and Tan D at three temperatures is shown in Fig. 9.

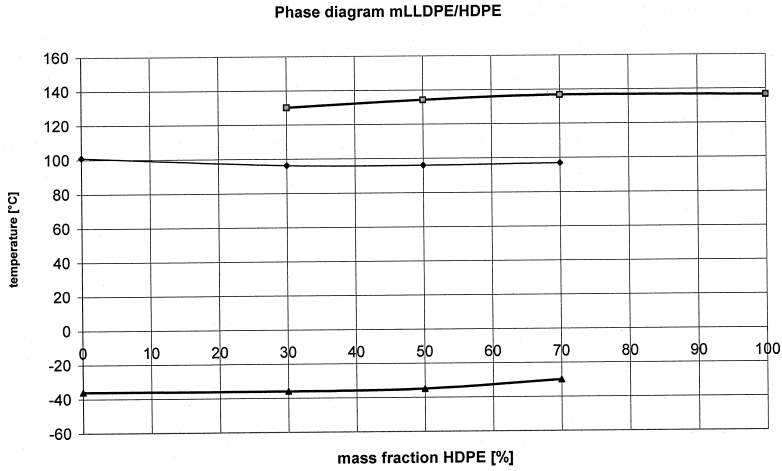

Figure 8. Phase diagram of mLLDPE and HDPE. Melting point from calorimetry, glass transition temperature from DMTA (maximum of the β-process of Tan D, the damping).

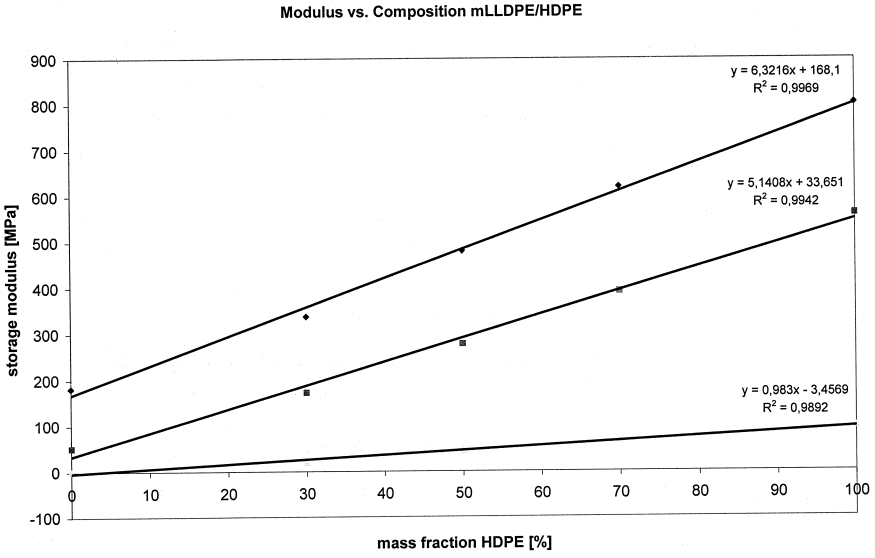

Figure 9. Composition-dependence of the storage modulus G' at –20°C (▲), 20°C (■) and 100°C (◆) in mLLDPE/HDPE blends. The curves can be described by a linear fit. The density grows linear with the HDPE content.

The System znLLDPE/LDPE:

There are the two melting endotherms of znLLDPE visible almost over the whole concentration range. LDPE shows only one melting transition which is also present in znLLDPE. The two polymers – miscible in the molten state and probably also in the amorphous state – crystallize at least partially separately, see Fig. 10.

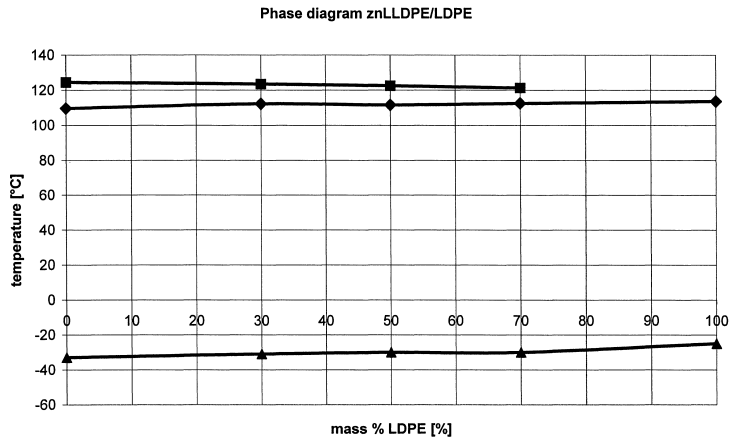

Figure 10.Phase diagram of znLLDPE/LDPE blends.

Fig. 11 shows a maximum of the storage modulus at a composition of about 70% w/w. The density at room temperature shows same behaviour, but much more pronounced.

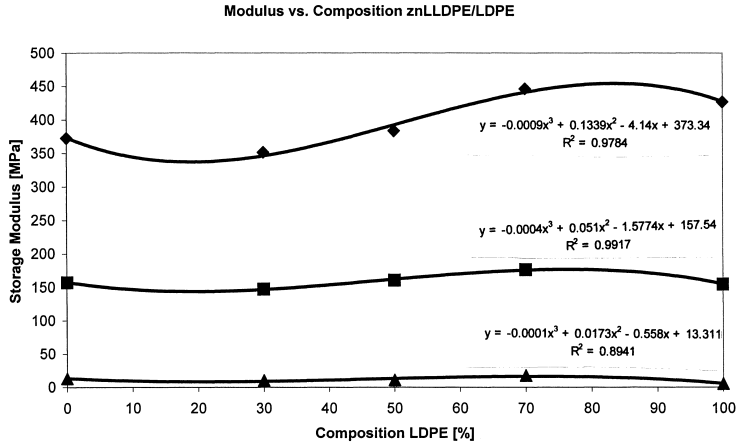

Figure 11. Composition-dependence of the storage modulus G' at –20°C (▲), 20°C (■) and 100°C (◆) in znLLDPE/LDPE blends.

The separate crystallization of the high melting population in znLLDPE was also observed by by R. S. Stein and coworkers [12] who showed that during the crystallization the volume is filled by LLDPE spherulites first. The LDPE crystallizes later within the earlier crystallized znLLDPE super structures. In our samples, however, there was an additional lower melting population present which seems to co-crystallize with LDPE. It seems that miscibility of the crystalline population melting around 110°C in the fractionation experiment causes higher crystallinity in the blend and hence a higher density and a higher storage modulus, see Table 3. α-, β-, and γ-transition of both polymers are very similar, except for the β-transition which is more prominent in znLLDPE.

The System znLLDPE/HDPE:

In contrast to the finding of Stein et al.[10] there are two endotherm transitions in znLLDPE (109°C, 124°C) but only one in HDPE (136°C). The lower transition vanishes with decreasing transition temperature before 50% HDPE is reached. The higher transition is shifted to higher temperatures with increasing HDPE-content indicating a co-crystallization of these populations. The phase diagram is shown in Fig. 12.

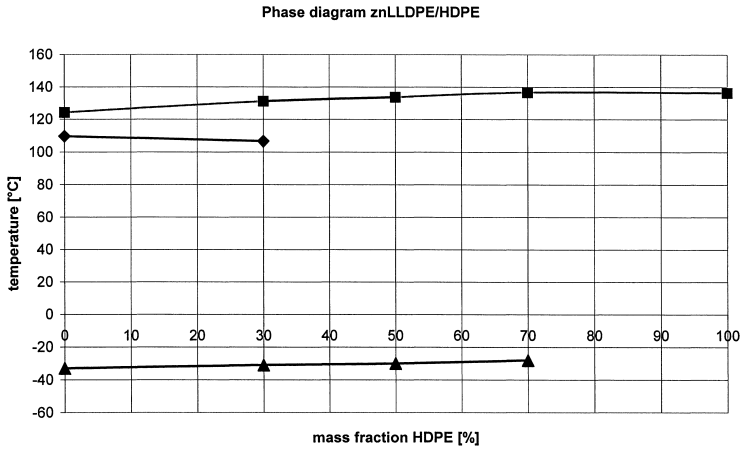

Figure 12. Phase diagram of znLLDPE/HDPE blends.

Co-crystallization has already been proved by Stein and coworkers in their extensive investigation[10-12] of mixtures of polyethylenes. In this case, however, it only is present in the higher melting crystalline population. The dynamic-mechanical spectrum shows a mixture of the two components and the composition dependence of the storage modulus at fixed

temperatures obeys a linear mixing rule with good accuracy and behaves very similar to the blends consisting of mLLDPE and HDPE, see Figs. 13 and 9.

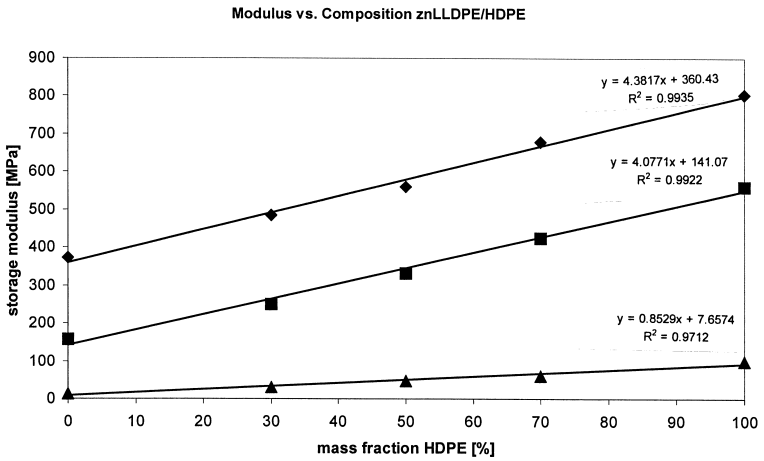

Figure 13. Composition-dependence of the storage modulus G' at –20°C (▲), 20°C (■) and 100°C (◆) in znLLDPE/HDPE blends.

The density grows linearly with HDPE content below 50% and becomes steeper at higher HDPE content.

Blends with PP

There is no interaction between the different types of PE and PP at any composition. Crystallization of the individual components is not affected by the presence of the second, and also the individual glass-transition temperatures are not influenced by the second component.

Conclusion

Both linear low density 1-octene copolymers, mLLDPE and znLLDPE, show the expected high branching content. The homopolymer HDPE is essential linear while the homopolymer LDPE shows a comparably high degree of non-uniform short-chain branching, see Table 2 and Figs. 2 and 3. For mLLDPE crystallinity and melting point increase with decreasing branching content within experimental error. That means that the branches are rather homogeneously distributed and they disturb the formation of highly regular crystalline phases. znLLDPE on the other hand appears to be a rather inhomogeneous copolymer with a

heterogeneous distribution of the short-chain branching. These differences in sequence distribution are related to the decrease in the linear growth rate of mLLDPE compared with znLLDPE[23]. Co-crystallization, known from blends of znLLDPE and HDPE through the investigations of Stein et al.[10], appears to be more influenced by the heterogeneity of the branching distribution and the nature of the copolymer than the branching content; Stein used a 1-butene copolymer as second component. It seems to be necessary that one of the components shows a good crystallizability and crystallizes first. If the second component contains chain populations with a comparable branching structure, they will co-crystallize. The second, more heterogeneously branched component then is able to crystallize in the already existing spherulitic lamellae. Hence, mLLDPE and LDPE co-crystallize and znLLDPE and LDPE do so only in the lower-melting structures while a higher melting population crystallizes independently.

The complexity of the LDPE structure is produced by the high-pressure synthesis which causes a high degree of heterogeneous branching along with a broad polydispersity. Apparently, there is no sequence of crystallite distribution. In this sense this homopolymer resembles the znLLDPE copolymer[24].

In the same way mLLDPE and HDPE have a high similarity in their regular structure and narrow molar mass distribution which support crystallization, although the higher the molar mass the smaller the rate of crystallization. But there are two crystalline populations present, one governed by HDPE and one governed by mLLDPE, which show some interaction since there is always a decrease of the melting point with increasing composition of the other component. The reason for no significant co-crystallization seems to be the comparably long – although fairly regular distributed – side chains on the copolymer which do not fit into the HDPE lamellae.

In all cases there seems to be a miscibility of the components in the amorphous phase. However, as can be shown by 13C-NMR[19], there are different amorphous phases which cannot be resolved by calorimetric or dynamic–mechanical experiments. Further problems arise from the resolution of the glass- transition in these experiments. A more detailed analysis of the amorphous phases will be subject of subsequent investigations. The interactions between mLLDPE and the other components appears to be stronger compared with those of znLLDPE. The result is an improvement of the mechanical properties. There is no general statement about miscibility of the different PEs possible, degree, length and distribution (depending on the used catalysts) of the branching are important as well as molar mass (at least in the low molar mass range).

Acknowledgement

Kirsten Schwark, Manfred Meyer and Dip. Chem. Ralf Woelke, Gerhard-Mercator-University, are greatly acknowledged for part of the thermal investigations.

References

[1] W. Kaminsky, M. Miri, H. Sinn, and R. Woldt, *Macromol Chem. Rapid Commun.*, **4**, 417 (1983)
[2] K. Shirayama, T. Okada, and S. Kita, *J. Polym. Sci.* A-2, **3**, 907 (1965)
[3] J. D. Hoffman, J. J. Weeks, *J. Res. Natl. Bur. Stand.* (U.S. A.) **66A**, 13 (1966)
[4] H. Krömer in: M. Hoffmann, H. Krömer, R. Kuhn, *Polymeranalytik II*, Stuttgart (1977) p. 179
[5] J. V. Seppäla *Polym Eng. & Sci.* **39**, 8 (1999)
[6] G. Strobl, *Macromolecules* **28**, 5827 (1995)
[7] G. Strobl, *J. Polym. Sci.* **18**, 1361 (1980)
[8] P. Starck, P. Lemhus, and J. V. Seppäla, *Polym Eng. & Sci.* **39**, 1444 (1999)
[9] R. S. Stein, F. B. Khambatta, F. P. Warner, T. Russell, A. Escala, and E. *Balizer J. Polym. Sci.; Polym. Phys. Ed.* **63**, 313 (1978)
[10] Shi-Rhu Hu, T. Kyu, and R. S. Stein, *J. Polym. Sci. B: Polym. Physics* **25**, 71 (1987)
[11] Shi-Rhu Hu, T. Kyu, and R. S. Stein, *J. Polym. Sci. B: Polym. Physics* **25**, 89 (1987)
[12] M. Ree, Thein, Kyu, and R. S. Stein, *J. Polym. Sci. B: Polym. Physics* **25**, 105 (1987)
[13] K. H. Illers, H. Breuer, *J. Coll. Sci.* **18**, 839 (1963)
[14] R. Kosfeld, J. Mansfeld, S. Schäfer, E. Schulz, *Rheol. Acta* **18**, 576 (1979)
[15] Z.-Q. Fan, F. Forlini, I. Tritto, P. Locatelli, M. C. Sacchi, *Macromol. Chem. Phys.* **195**, 3889 (1994)
[16] K. Schmidt-Rohr, H. W. Spiess, *Macromolecules* **24**, 5288 (1991)
[17] K. H. Illers, *Koll Z., Z. Polymere* **231**, 622 (1969)
[18] H. Boyd, Polymer **26**, 1123 (1985)
[19] L. Hillebrand, A. Schmidt, A. Bolz, M. Hess and W. S. Veeman, *Macromolecules* **31**, 5010 (1998)
[20] L. Wild, T. R. Ryle, D. C. Knobeloch, and I. R. Peat, *J. Polym. Sci.; Polym. Phys.* **20**, 441 (1982)
[21] T. Albrecht, G. R. Strobl, *Macromolecules* **28**, 5827 (1995)
[22] G. R. Strobl, M. J. Schneider, I. G. Voigt-Martin, *J. Polym. Sci.* **18**, 1361 (1980)
[23] J. Wagner, K. Monar, P. Phillips, *Proceedings Ann. Techn. Meeting SPE*, Pittsburg !998)
[24] W. S. Lambert, P. J. Phillips, *Polymer* **37**, 3585 (1996)